

---

# ENERGY BALANCE MODEL AS REAL EVAPOTRANSPIRATION ESTIMATOR WITH SATELLITE AND METEOROLOGICAL DATA

---

Sebastián Anibal Gavilán, Juan Ignacio Pastore, Ignacio Quignard, Néstor Damián Marasco and Pablo Gilberto Aceñolaza

## SUMMARY

Evapotranspiration (ET) is the process whereby water present in the soil is transferred to the atmosphere as vapor. ET is one of the most important fluxes in the hydrological cycle, with estimates of more than 60% of precipitation returning to the atmosphere through ET. Different methods based on weather information have been used to estimate reference ET ( $ET_0$ ), but they provide regional nature estimates, since  $ET_0$  expresses only the evaporating power of the atmosphere. The ET that actually takes place from a given plant cover is known as real ET ( $ET_R$ ) and its estimation is usually more complex since it requires information about the current state of the vegetation. Satellite

information is an attractive tool to obtain data on vegetation and soil moisture, which can be complemented with meteorological information. This paper proposes and evaluates an energy balance model to calculate  $ET_R$  using data from satellite imagery and meteorological stations. The model is based on SEBAL (surface energy balance algorithm for land), which was modified for automatically selecting/classifying pixels by thresholds. The generated model was tested in two typical wheat/soy bean farming areas of Argentina. The results showed an appropriate segregation of the dominant soil cover types and a high concordance of obtained data with those present in the literature.

## Introduction

Advances in information technologies have facilitated the storage of large amounts of data in the last years (Tan *et al.*, 2005). However, the methods to retrieve useful information from those sources have not evolved at the same rate. Possibly, the traditional tools and techniques for data analysis may not be appropriate or sufficient for processing the information influx (Sumathi and Sivanandam, 2006). An important amount of data is continually generated by satellites orbiting the Earth. These instruments acquire different types of territorial information, with large spatial/temporal cover from oceans, the atmosphere

and land surface (Tan *et al.*, 2005). Likewise, the information obtained from meteorological stations provides the real measure of the environmental conditions at a given site. Combining both information fluxes is a challenge posed by the use of modern technologies for data gathering and processing. Thus, it becomes a tool for transforming satellite data into useful information for monitoring environmental variables (Lillesand *et al.*, 2014). Here, we develop and evaluate a model that uses data from remote sensors and weather stations to estimate real evapotranspiration (ETR) at pixel scale.

Evapotranspiration (ET) is the process that describes water transport from the different

land surfaces (soil, vegetation, water bodies, etc.) to the atmosphere (Njoku and Njoku, 2014). This process is divided (Stancalie and Nertan, 2012) into a physical component (direct evaporation) and a biological component (transpiration occurring in the stomatal pores of plants). It has been estimated that more than 60% of precipitation returns to the atmosphere in the form of ET, being one of the most important fluxes in the hydrological cycle (Zeng *et al.*, 2012). The energy used for ET, referred to in the literature as latent heat flux, is one of the main consumptions of solar energy by the land surface (Yao *et al.*, 2013). This phenomenon is strongly associated with meteorological variables

(temperature, humidity and wind speed), vegetative vigor of plants and soil available moisture (Allen, 2006; Atchley and Maxwell, 2011). The latter variable is a limiting factor, even when the remaining variables favor the ET process (Mausser and Schadlich, 1998).

There are two approaches (Allen, 2006) to deal with the ET concept: ET of the reference crop ( $ET_0$ ) and real ET of the crop ( $ET_R$ ).  $ET_0$  indicates the amount of water used by a crop (reference crop) under determined conditions. UN Food and Agriculture Organization (FAO) experts defined the hypothetical reference crop as an area cultivated with alfalfa (*Medicago sativa* L.) and raygrass (*Lolium*

---

## KEYWORDS / Energy Balance / Hydrological Variable Modeling / Real Evapotranspiration /

Received: 10/17/2018. Modified: 07/09/2019. Accepted: 07/11/2019.

**Sebastián Gavilán.** Doctor in Agrarian and Forestry Sciences, Universidad Nacional de La Plata (UNLP), Argentina. Doctoral Fellow, Centro de Investigaciones Científicas y Transferencia de Tecnología a la Producción (CICYTTP-CONICET), Entre Ríos, Argentina. e-mail: gavilan@agro.uba.ar

**Juan I. Pastore.** Doctor in Electronics, Universidad Nacional de Mar Del Plata, Argentina. Researcher, UNLP, Argentina. e-mail: jpastore@fi.mdp.edu.ar

**Ignacio Quignard.** Biologist and Specialist in Remote Sensing, Teaching assistant, Regional Center of Geomatics (CeReGeo), Universidad Autónoma de Entre

Ríos, Argentina. e-mail: ignacio-quignard@gmail.com

**Néstor D. Marasco.** Electronic Engineer, Universidad Tecnológica Nacional (UTN), Argentina. Professor, UTN, Argentina.

**Pablo G. Aceñolaza** (Corresponding autor). Biologist and Doctor in Biological Sciences, Universidad de Tucumán, Argentina. Researcher and Professor,

Universidad Nacional de Entre Ríos (UNER), Argentina. Address: Centro de Investigaciones Científicas y Transferencia de Tecnología a la Producción. CICYTTP-CONICET, Materi y España (3100) Diamante, Entre Ríos, Argentina and Facultad de Ciencias Agropecuarias, UNER, Argentina. e-mail: acenolaza@gmail.com.

## MODELO DE BALANCE DE ENERGÍA PARA ESTIMAR EVAPOTRANSPIRACIÓN REAL A PARTIR DE INFORMACIÓN SATELITAL Y METEOROLÓGICA

Sebastián Anibal Gavilán, Juan Ignacio Pastore, Ignacio Quignard, Néstor Damián Marasco y Pablo Gilberto Aceñolaza

### RESUMEN

La evapotranspiración (ET) es el proceso mediante el cual el agua presente en el suelo se transfiere a la atmósfera en forma de vapor. ET es uno de los flujos más importantes en el ciclo hidrológico, con estimaciones de más del 60% de las precipitaciones que regresan a la atmósfera a través de ET. Se han utilizado diferentes métodos basados en información meteorológica para estimar ET de referencia ( $ET_0$ ), pero proporcionan estimaciones de la naturaleza regional, ya que  $ET_0$  expresa solo el poder de evaporación de la atmósfera. La ET que realmente tiene lugar a partir de una cobertura vegetal dada se conoce como ET real ( $ET_R$ ) y su estimación suele ser más compleja ya que requiere información sobre el estado actual de la vegetación. La información satelital es una herramienta atractiva

para obtener datos sobre la vegetación y la humedad del suelo, que se puede complementar con información meteorológica. Este documento propone y evalúa un modelo de balance de energía para calcular  $ET_R$  utilizando datos de imágenes satelitales y estaciones meteorológicas. El modelo se basa en SEBAL (algoritmo de balance de energía superficial para tierra) que fue modificado, en el presente trabajo, para seleccionar/clasificar automáticamente píxeles por umbrales. El modelo generado se probó en dos zonas típicas del cultivo de trigo y soja de Argentina. Los resultados mostraron una segregación apropiada de los tipos de cobertura del suelo dominante y una alta concordancia con los datos obtenidos con aquellos presentes en la literatura.

## MODELO DE BALANÇO DE ENERGIA PARA ESTIMAR A EVAPOTRANSPIRAÇÃO REAL DE DADOS SATÉLITES E METEOROLÓGICOS

Sebastián Anibal Gavilán, Juan Ignacio Pastore, Ignacio Quignard, Néstor Damián Marasco e Pablo Gilberto Aceñolaza

### RESUMO

A evapotranspiração (ET) é o processo pelo qual a água presente no solo é transferida para a atmosfera como vapor. ET é um dos fluxos mais importantes no ciclo hidrológico, com estimativas de mais de 60% de precipitação retornando à atmosfera através de ET. Diferentes métodos baseados em informações meteorológicas têm sido usados para estimar a referência ET ( $ET_0$ ), mas fornecem estimativas de natureza regional, uma vez que  $ET_0$  expressa apenas o poder de evaporação da atmosfera. O ET que realmente ocorre a partir de uma determinada cobertura vegetal é conhecido como ET real ( $ET_R$ ) e sua estimativa é geralmente mais complexa, uma vez que requer informações sobre o estado atual da vegetação. A informação de satélite é uma ferramenta

atractiva para obter dados sobre a umidade da vegetação e do solo, que pode ser complementada com informações meteorológicas. Este artigo propõe e avalia um modelo de balanço de energia para calcular o  $ET_R$  usando dados de imagens de satélite e estações meteorológicas. O modelo é baseado no SEBAL (algoritmo de equilíbrio de energia superficial para terra), que foi modificado para selecionar/classificar automaticamente pixels por limiares. O modelo gerado foi testado em duas áreas de cultivo de trigo e soja da Argentina. Os resultados mostraram uma adequada segregação dos tipos de cobertura do solo dominante e uma alta concordância com os dados obtidos com os presentes na literatura.

*multiflorum* Lam.) of 12cm height, without water deficit and growing under no nutrition or health limiting conditions (Allen, 2006). Since this is a hypothetical crop, this variable is mostly related to climate, because it expresses the evaporating power of the atmosphere (Allen *et al.*, 2003). However,  $ET_0$  is a theoretical concept that assumes water availability and plant growth states that do not often occur in the real situation. Real evapotranspiration ( $ET_R$ ), sometimes named crop evapotranspiration ( $ET_C$ ), involves evaporation from the soil and transpiration that really occurs in a given period under conditions different from those of the reference crop (Allen *et al.*, 2007). The

relationship between  $ET_0$  and  $ET_R$  is expressed by a dimensionless coefficient known as *kc*, which incorporates phenological and management factors (Allen *et al.*, 2015).

Since direct measurement of ET is not easy and requires costly equipment, different methods have been developed to estimate the amount of water that is lost through ET. These methods can be classified as empirical (Thornthwaite, 1948; Blaney *et al.*, 1952) or physics-based (e.g. Penman, 1948; Monteith, 1981 and FAO Penman Monteith, in Allen (2006)). The FAO Penman Monteith method is considered the standard model for estimating ET in agriculture (Zeheke and Wade, 2012). This model is

useful to estimate  $ET_0$  as it requires only weather data for the calculations (Allen, 2006). Then, to obtain an actual measure of the water consumed by ET, it is necessary to incorporate some measurements of the current vegetation state into the model. A feasible alternative for solving this problem is to use satellital information to complement the models based on meteorological data (Bastiaanssen *et al.*, 1998a). Here, we present and evaluate a model using the FAO Penman Monteith equation to calculate  $ET_0$ , then it calculates the ET fraction (similar to *kc*) using an energy balance model. This model is based on the surface energy balance algorithm for land (SEBAL) and incorporates

a method for automatically selecting pixels by thresholds. Moreover, an equation recommended by the International Committee on Weights and Measures (CIPM) to calculate air density is incorporated.

### Materials and Methods

#### Study area

The application of the surface energy balance model was carried out in two test sites (Figure 1). The first one in the south of the province of Buenos Aires (Lobería, 38°11'1.47"S, 58°52'22.89"W) and the second one in the Paraná Department, Entre Ríos Province (31°51'14.26"S, 60°28'18.87"W); both in

Argentina. For the Lobería area (application 1), meteorological data (Table I) were used from Agricultural School No. 1, located 7.8km from the studied site (38°7'0.44"S, 58°51'8.37"W). For Paraná area (application 2), meteorological data were used from the Paraná Station, National Institute of Agricultural Technology (EEA-INTA), located 6.1km from the center of the analyzed image (31°49'51.56"S, 60°31'8.40"W).

#### Meteorological and satellite data

Landsat 5TM images were downloaded from the GLOVIS server provided by the USGS-NASA (USGS 2016). For Lobería, a subset of the image was generated (date 29/01/2009; 225/086 path/row), its area was 2.34km<sup>2</sup> (1.54×1.52km). For Paraná site, image (date 23/01/2011; 227/082 path/row) an area of 13.6km<sup>2</sup> (4.7×2.9km) was used. These sites were chosen within a coverage area of the meteorological station demarcated by a buffer of 10km radius.

TABLE I  
METEOROLOGICAL INFORMATION FROM EEA INTA PARANÁ

Application	Date	Mean temp. (°C)	ET <sub>0</sub> * (mm/day)	Wind speed (m.s <sup>-1</sup> )	Relative humidity (%)
Lobería	29/01/2009	20.95	4.46	8.1	65
Paraná	23/01/2011	28.4	6.3	5.4	61

The model requires, as inputs, daily means of temperature (°C), wind speed (m·s<sup>-1</sup>), relative humidity (%), also maximum and minimum values of those variables and an estimate of the reference evapotranspiration (ET<sub>0</sub>) calculated with the FAO-Penman-Monteith method.

#### Model description

To compute parameters that compose the model we first present the energy balance equation (EBE), and then we develop the equations and procedures that structure the whole model.

#### Energy Balance Equation (EBE)

$$\lambda ET (W \cdot m^{-2}) = R_n - G - H$$

This equation calculates the latent heat flux (ET), the energy used for ET, as a residual, which is obtained by subtracting the soil heat flux (G) and the sensible heat flux (H) from the Net Radiation (R<sub>n</sub>) (Li *et al.*, 2005; Sánchez *et al.*, 2008).

#### Net Radiation (R<sub>n</sub>)

$$R_n = R_{s\downarrow} - R_{s\uparrow} + R_{L\downarrow} - R_{L\uparrow}$$

Net radiation is the term of highest magnitude within the EBE and represents the amount of energy available for physical and biological processes occurring on the land surface. Its calculation requires a balance between the outgoing (↑) and incoming (↓) energy fluxes for the shortwave (S= 0.25 to 3μm) and longwave (L= 3 to

100μm) radiation fractions (Stancalie and Nertan 2012). This balance can be made from satellite data using the following equation (Bastiaanssen *et al.*, 1998a):

$$R_n = (1-\alpha) R_{s\downarrow} + R_{L\downarrow} - R_{L\uparrow} - (1-\epsilon_0) R_{L\downarrow}$$

The energy corresponding to incoming shortwave radiation (R<sub>s↓</sub>) that reaches the earth's surface is that which has still not been returned to the atmosphere through reflection. This reflected energy is known as surface albedo (α) and depends on the cover type (Chuvieco, 2010). To calculate α, the following equation was used (Robinove, 1981; Duguay and LeDrew, 1992):

$$\alpha = (\alpha_{toa} - \alpha_{path\_radiance}) / \tau_{sw}^2$$

where albedo at the top of the atmosphere (α<sub>toa</sub>) is calculated from reflectivity (ρ<sub>λ</sub>) of each band, except for the thermal band (Bastiaanssen *et al.*, 1998a):

$$\alpha_{toa} = \sum (\omega_\lambda \times \rho_\lambda)$$

To do this, participation of mean solar exo-atmospheric irradiance of each band should be calculated (ESUN<sub>λ</sub>) using its weighting coefficient ω<sub>λ</sub>:

$$\omega_\lambda = ESUN_\lambda / \sum ESUN_\lambda$$

The calculation of the reflectivity of each band requires converting the digital numbers (DN) to spectral radiance values (L<sub>λ</sub>) using the satellite calibration constant (Chander and Markham, 2003). Then, reflectivity is calculated for each band, as follows:

$$\rho_\lambda = (\pi \times L_\lambda) / (ESUN_\lambda \times \cos\theta \times d_r^2)$$

where θ: solar incidence angle and d<sub>r</sub>: the earth-sun distance, calculated using the Julian Day

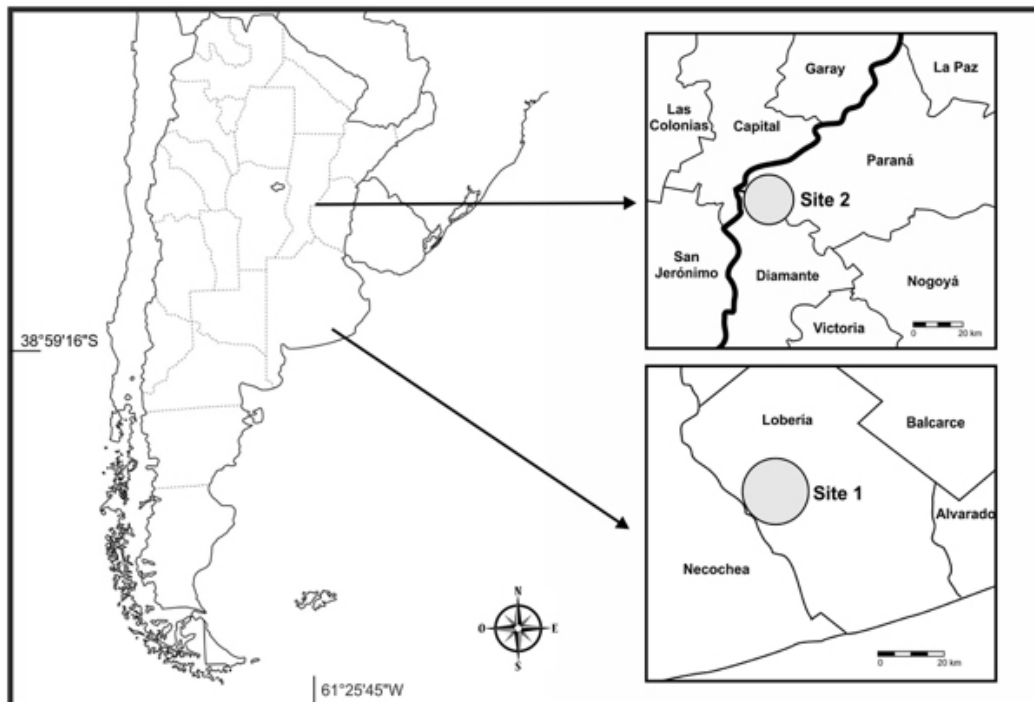


Figure 1. Study area. Lobería site (application 1) and Paraná site (application 2).



(JD) (Duguay and LeDrew, 1992; Chuvieco, 2010).

Furthermore,  $\alpha_{\text{path\_radiance}}$  is a mean fraction of the incoming solar radiation that is back-scattered before it reaches the earth's surface (Bastiaanssen, 2000). Atmospheric transmissivity ( $\tau_{\text{sw}}$ ) is a dimensionless value that indicates the incoming radiation fraction that actually reaches the earth's surface. This phenomenon occurs due to absorption and diffusion of radiation by particles suspended in the atmosphere. In this model, this fraction is calculated as a function of the height of the site ( $z$ ) (Allen, 2006):

$$\tau_{\text{sw}} = 0,75 + 2 \times 10^{-5} \times z$$

The term  $R_{\text{c}\downarrow}$  refers to the direct and diffuse solar radiation flux that actually reaches the earth's surface, and is measured in  $\text{W}\cdot\text{m}^{-2}$ :

$$R_{\text{c}\downarrow} = G_{\text{sc}} \times \cos_s \times d_r \times \tau_{\text{sw}}$$

$G_{\text{sc}}$  is the solar constant ( $1367\text{W}\cdot\text{m}^{-2}$ ) and the remaining components are the same factors used for the calculation of reflectances and albedo at the top of the atmosphere (Duffie *et al.*, 2013).

The next term, necessary to solve the net radiation equation, is the outgoing longwave radiation ( $R_{\text{L}\uparrow}$ ) emitted from the earth's surface. To obtain this parameter it is necessary to compute the vegetation indices NDVI (normalized difference vegetation index) and SAVI (soil-adjusted vegetation index). Then, LAI (leaf foliar area index) is calculated based on SAVI (Bannari *et al.*, 1995). Two emissivity values are computed: Thermal emissivity within the spectral range of band 6 ( $\epsilon_{\text{NB}}$ ) and Emissivity in the broad thermal spectrum ( $\epsilon_0$ ). To calculate emissivity values, the following equations and logical operations are used (Allen *et al.*, 2002):

$$\epsilon_{\text{NB}} = 0,97 + 0,0033 \times \text{LAI} \quad \text{if LAI} < 3$$

$$\epsilon_{\text{NB}} = 0,98 \quad \text{if LAI} \geq 3$$

$$\epsilon_0 = 0,95 + 0,01 \times \text{LAI} \quad \text{if LAI} > 3$$

$$\epsilon_0 = 0,98 \quad \text{if LAI} \geq 3$$

The following step consists of computing radiation emitted by the earth in the thermal spectrum ( $R_{\text{c}}$ ), correcting the values of radiance of band 6 ( $L_6$ ) (Wukelic *et al.*, 1989):

$$R_{\text{c}} = (L_6 - R_p / \tau_{\text{NB}}) - (1 - \epsilon_{\text{NB}}) \times R_{\text{sky}}$$

To solve this equation, three parameters related to the state of the atmosphere are necessary: Thermal radiance emitted by the atmosphere in the direction of the satellite ( $R_p$ ), air transmissivity ( $\tau_{\text{NB}}$ ) and thermal radiance emitted by the atmosphere in the direction of the earth ( $R_{\text{sky}}$ ) (Barsi *et al.*, 2003). Values for  $R_p$  and  $\tau_{\text{NB}}$  require using a simulation model for atmospheric radiation transfer (e.g. MODTRAN; Berk *et al.*, 1999). In extreme cases of lack of data for these terms, fixed values 0, 1 and 0 are assigned to parameters  $R_p$ ,  $\tau_{\text{NB}}$  and  $R_{\text{sky}}$ , respectively (Allen *et al.*, 2002). This converts  $R_{\text{c}}$  into an uncorrected radiance of band 6. Not correcting  $L_6$  results in an underestimation of surface temperature  $T_s$  in  $5^\circ$ . However, in further steps of this model, a function must be generated to determine the difference between surface temperature and air temperature (Bastiaanssen *et al.*, 1998b). For this reason, the error of  $L_6$  estimation has a low effect on the final value of ET calculated by the model (Allen *et al.*, 2002).

Once  $R_{\text{c}}$  is calculated, surface temperature ( $^{\circ}\text{K}$ ) is obtained from the equation based on Planck's law:

$$T_s = K_2 / \ln((\epsilon_{\text{NB}} \times K / R_{\text{c}}) + 1)$$

where  $K_1$  ( $607,76\text{mW}\cdot\text{cm}^{-2}\cdot\text{sr}^{-1}\cdot\mu\text{m}^{-1}$ ) and  $K_2$  ( $1260,56\text{mW}\cdot\text{cm}^{-2}\cdot\text{sr}^{-1}\cdot\mu\text{m}^{-1}$ ) are constants for Landsat 5 band 6 (Markham and Barker, 1986). To complete this step, outgoing long wave radiance ( $R_{\text{L}\uparrow}$ ) is calculated using Stefan-Boltzmann's equation:

$$R_{\text{L}\uparrow} = \epsilon_0 \times \sigma \times T_s^4$$

where  $\sigma$  is the Stefan-Boltzmann constant ( $5,67 \times 10^{-8}\text{W}\cdot\text{m}^{-2}\cdot\text{K}^{-4}$ ).

To complete the calculation of the parameters necessary for solving Rn equation, incoming long wave radiance ( $R_{\text{L}\downarrow}$ ) is calculated:

$$R_{\text{L}\downarrow} = 0,85 (-\ln \tau_{\text{sw}})^{0,09} \times \sigma \times T_{\text{cold}}^4$$

To solve this equation, the  $T_{\text{cold}}$ , referred to mean temperature of cold pixels is calculated. For this, a process for selecting 'cold' and 'hot' pixels is conducted, which is explained below in the calculation of sensible heat flux (H).

#### Soil heat flux (G)

Soil heat flux (G) refers to the energy stored in the soil and vegetation and is transferred through conduction. To obtain this parameter, the G/Rn relation is computed using the following equation (Bastiaanssen *et al.*, 1998b):

$$\frac{G}{R_n} = \frac{T_s}{\alpha} \times (0,0038 \times \alpha + 0,0074 \times \alpha^2) \times (1 - 0,98 \times \text{NDVI}^4)$$

where  $T_s$ : surface temperature ( $^{\circ}\text{C}$ ) obtained from the image on band 6 of the sensor and,  $\alpha$ : surface albedo. Then, knowing the values for  $R_n$ , G must be solved for.

#### Sensible heat flux (H)

H represents the energy fraction that heats the air through convection and conduction. This parameter is the most difficult to model and is usually the factor differentiating the diverse models available for remote sensors. In SEBAL, the driver of this energy flux is the temperature difference between the soil surface and the air ( $dT$ ) (Bastiaanssen, 2000). Parameter  $dT$  is estimated from a linear function calculated with the information of the cold and hot pixels. These pixels correspond to contrasting energy balance situations within the image, where H and  $\lambda$  ET are assumed as known (Bastiaanssen *et al.*, 1998a; Allen *et al.*, 2002).

Here, we incorporate logical operators that impose conditions for automating the pixel selection process. The 'cold'

pixels represent a wet soil surface, with irrigated crops and good plant cover. The selection condition is that surface temperature should be between the 10<sup>th</sup> and 20<sup>th</sup> percentiles of its distribution and NDVI should be between 0.7 and 0.8. 'Hot' pixels are representative of a dry surface with low plant cover, where ET is close to 0. It is assumed that surface temperature in cold pictures is similar to air temperature, whereas the maximum difference between them is given by hot pixels (Allen *et al.*, 2002). The condition for selecting hot pixels is that surface temperature should be between the 80<sup>th</sup> and 90<sup>th</sup> percentiles and the NDVI between 0.2 and 0.3.

In 'cold' pixels, it is assumed that ET is 5% higher than  $ET_0$ ; therefore, sensible heat flux is defined as:

$$H_{\text{cold}} = R_n - G - 1,05 \times \lambda ET_0$$

For 'hot' pixels, where there is scarce vegetation and humidity, it is assumed that there is no ET, hence:

$$H_{\text{hot}} = R_n - G$$

Then,  $dT$  is computed for the selected pixels:

$$dT_{\text{cold/hot}} = (H_{\text{cold/hot}} \times r_{\text{ah}}) / (\rho \times C_p)$$

For this, it is necessary to obtain the aerodynamic resistance to heat transport ( $r_{\text{ah}}$ ), air density ( $\rho$ ) and  $C_p$ , the specific heat of the air ( $1004\text{J}\cdot\text{kg}^{-1}\cdot\text{K}^{-1}$ ). The resistance  $r_{\text{ah}}$  is related to wind speed ( $u_x$ ) and to the friction of the air layer that interacts with the surface ( $Z_{\text{om}}$ ). In principle, its magnitude is calculated for conditions of neutral atmosphere stability. Then, the instability conditions are simulated via a process of iterations (Bastiaanssen *et al.*, 1998a).

To obtain the parameter  $\rho$ , an equation recommended by the International Committee for Weights and Measures (CIPM) was introduced: CIPM 1981/91 (Davis, 1992):

$$\rho = \frac{p \times M_a}{Z \times R \times T} \times [1 - x_v \times (1 - (M_v / M_a))]$$

where p: atmospheric pressure (101325 Pascals),  $M_a$ : molar mass of dry air (0.0289635 kg·mol<sup>-1</sup>), Z: dimensionless compressibility factor, R: molar constant of gases (8.31451 J·kmol<sup>-1</sup>), T: air temperature in °K,  $X_v$ : dimensionless molar fraction of vapor and,  $M_v$ : molar mass of water vapor (0.0180154 kg·mol<sup>-1</sup>).

Once the difference in temperature for the selected pixels is computed, a linear regression plot is performed between dT and Ts. The coefficients of the trend line of this regression (slope and intercept) will be used to compute dT for all the pixels of the image as a function of their surface temperature:

$$dt = b + a \times Ts$$

When all the parameters are calculated for all the image pixels, the following equation is solved:

$$H = (\rho \times C_p \times dT) / \tau_{ah}$$

*Latent heat flux ( $\lambda ET$ )*

As already mentioned,  $\lambda ET$  (W·m<sup>-2</sup>) is calculated as a residual of the energy balance. However, the previously computed energy fluxes (H, G and Rn) are instantaneous; hence, the estimations must be extrapolated to daily values. To solve this problem, the concept of evaporative fraction is used, which is the energy used for the evaporation process over the total of energy available for the process (Brutsaert and Sugita, 1992):

$$\Lambda_{Inst} = \frac{\lambda ET}{\lambda ET + H} = \frac{\lambda ET}{Rn + G}$$

Then, assuming that evaporative fraction is constant along the day ( $\Lambda_{Inst} = \Lambda_{24hs} \approx Kc$ ), daily values of real ET (ETr) can be obtained using the following equation:

$$ETr \text{ (mm/day)} = ET_0 \times \Lambda_{24h}$$

*Model evaluation*

Two proofs of the model were carried out to evaluate its results. When moving from

Lobería (application 1) to Paraná (application 2), the number of types of ground cover and the number of pixels in the image were increased.

To evaluate the results produced by the model, the estimated Kcs were compared with the bibliographic ones for each type of coverage. To do this, the pixels of the selected images were classified. The subscene of the Lobería area, comprises a region with an irrigation pivot and a field bordering a stubble. The image of Lobería was classified by clusters based on the NDVI and the surface temperature derived from band 6 of the satellite. From this classification the pixels were grouped within the classes 'Irrigation' and 'Stubble' (Table II).

For the Paraná area (application 2), image pixels were classified into five land cover types that were generated through two classification stages. The first stage involved a supervised classification based on the visual analysis of the image, which originated three classes (crop, bare soil and natural vegetation; Chuvieco, 2010). The second stage included a classification by clusters using the k-means algorithm on NDVI values, surface temperature and the three classes generated during the first stage as classification variables. The aim of this second stage was to split vegetation types in six clusters. Clusters 5 and 6, were unified as 'Bare soil' class. For vegetation types, a higher NDVI refers to higher vegetation vigor and a lower Ts means a better hydric condition. For this reason, the classes 'Natural vegetation' and 'Crop' were subdivided into '+' for pixels of best vegetation condition and '-' for those of worst conditions. Then, different Kc values for each class (theoretical Kc) were selected from the literature (Allen 2006) (Table III).

After verifying the normality and homoscedasticity assumptions, an ANOVA was performed to evaluate the presence of significant differences in the mean ETr values of the classes.

TABLE II  
COMPOSITION OF THE FINAL CLASSES AND VALUES OF THEORETICAL Kc ASSIGNED IN LOBERÍA (APPLICATION 1 AREA)

Cluster	NDVI	Temp (°C)	Final class	Theoretical Kc
1	0.5364	33.2109	Natural veg -	0.3
2	0.8128	28.2579	Crop +	1.2
3	0.7057	30.1416	Crop -	0.9
4	0.5673	31.6689	Natural veg +	0.6
5	0.3907	35.3837	Bare soil	0.1

TABLE III  
COMPOSITION OF THE FINAL CLASSES AND VALUES OF THEORETICAL Kc ASSIGNED IN PARANÁ (APPLICATION 2 AREA)

Cluster	NDVI	Temp (°C)	Final class	Theoretical Kc
1	0.66	23.20	Irrigation	1.2
2	0.08	30.71	Stubble	0.2

$$H_0: \mu Kc(\text{Class A}) = \mu Kc(\text{Class B}) = \mu Kc(\text{Class C})$$

$$H_1: \mu Kc(\text{Class A}) \neq \mu Kc(\text{Class B}) \neq \mu Kc(\text{Class C})$$

Then, the correspondence of the theoretical Kc values with the Kc estimated by the model was tested. To do this, the probability of obtaining a Kc value equal to the theoretical one for a population that has the distribution parameters of the Kc of each class (mean and variance) was calculated with a t test.

$$H_0: \mu Kc(\text{Class A}) = \mu Kc(\text{Teórico Class A})$$

$$H_1: \mu Kc(\text{Class A}) \neq \mu Kc(\text{Teórico Class A})$$

Finally, the model ability to detect changes in vegetation state and soil hydric condition was evaluated for Paraná area (application 2). For this purpose, a simple linear regression analysis was performed for the two satellite variables related to NDVI and surface temperature.

## Results

For Lobería area (application 1), the ANOVA produced a p-value that remained outside the acceptance zone of the null hypothesis (Table IV); the same result was obtained in Paraná area (Table V).

For Lobería land coverage, the p-value associated with the

TABLE IV  
ANALYSIS OF VARIANCE FOR THE EFFECT OF CLASSES ON ETr FOR LOBERÍA REGION (APPLICATION 1)

FV	Sum sq	D.F.	F value	p-value
Class	13.615	1	810.8	<2e-16
Residuals	1.041	62		

Significance level  $\alpha = 0.05$

TABLE V  
ANALYSIS OF VARIANCE FOR THE EFFECT OF CLASSES ON ETr FOR PARANÁ REGION (APPLICATION 2)

FV	Sum sq	D.F.	F value	p-value
Class	64557.21	4	25688.37	<0.0001
Residuals	9405.87	14971		

Significance level  $\alpha = 0.05$

one parameter t-test was lower than the significance level ( $\alpha=0.05$ ) for the 'Irrigation' class and higher for the 'Stubble' class (Table VI). However, the mean value estimated in each class is within the 25<sup>th</sup> and 75<sup>th</sup> percentiles (Table VI, Figure 2).

For the Paraná region (application 2), p values associated with the statistic do not fall in the rejection region of the null hypothesis for any of the classes (Table VII, Figure 3).

Regression analysis between NDVI and the calculated ETr, shows a positive linear relationship between these variables ( $p<0.0001$ ),

although with a low adjustment level ( $R^2=0,37$ ) (Table VIII, Figure 4).

Finally, regression analysis between surface temperature and the calculated ETr also showed a significant, although opposite, linear relationship between these variables, but with high adjustment ( $R^2=0,91$ ) (Table IX, Figure 5).

### Discussion

The ANOVA that evaluated the effect of classes on ETr yielded a lower value at a significant level of 0.05 for both areas studied. This suggests the rejection of the hypothesis

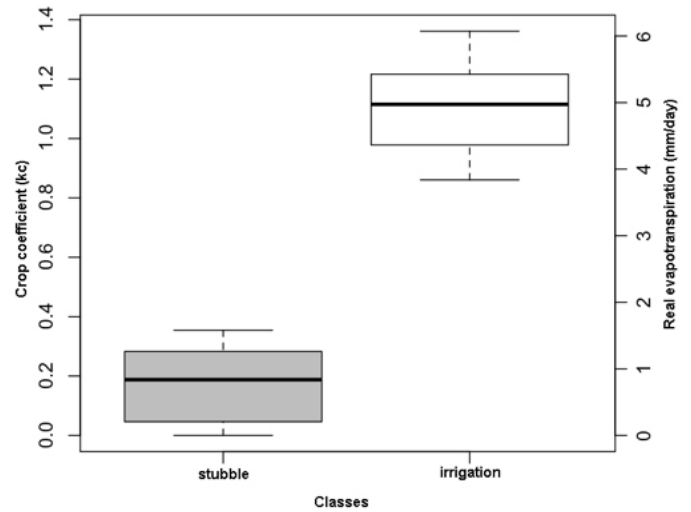


Figure 2. Kc and ETr Box plot for each classes in Lobería region (application 1).

TABLE VI  
DESCRIPTIVE STATISTICS OF THE Kc OF THE CLASSES IN LOBERÍA REGION (APPLICATION 1), p VALUE ASSOCIATED WITH THE THEORETICAL Kc

Class	Mean	S.D.	Var(n)	P(25)	P(75)	Theoretical Kc	p-value
Irrigation	1.13	0.15	0.018	0.978	1.24	1.2	0.0206
Stubble	0.17	0.12	0.015	0.05	0.28	0.2	0.2437

Significance level  $\alpha=0.05$

TABLE VII  
DESCRIPTIVE STATISTICS OF THE Kc OF THE CLASSES. P VALUE ASSOCIATED WITH THE THEORETICAL Kc. PARANÁ REGION (APPLICATION 2 AREA)

Class	Mean	S.D.	Var(n)	P(25)	P(75)	Theoretical Kc	p-value
Crop +	1.19	0.12	0.02	1.12	1.29	1.2	0.528
Crop -	0.88	0.13	0.02	0.78	0.98	0.9	0.556
Ground	0.07	0.11	0.01	0.00	0.12	0.1	0.583
Nat.veg. +	0.62	0.14	0.02	0.52	0.72	0.6	0.443
Nat.veg. -	0.28	0.12	0.02	0.19	0.36	0.3	0.556

Significance level  $\alpha=0.05$

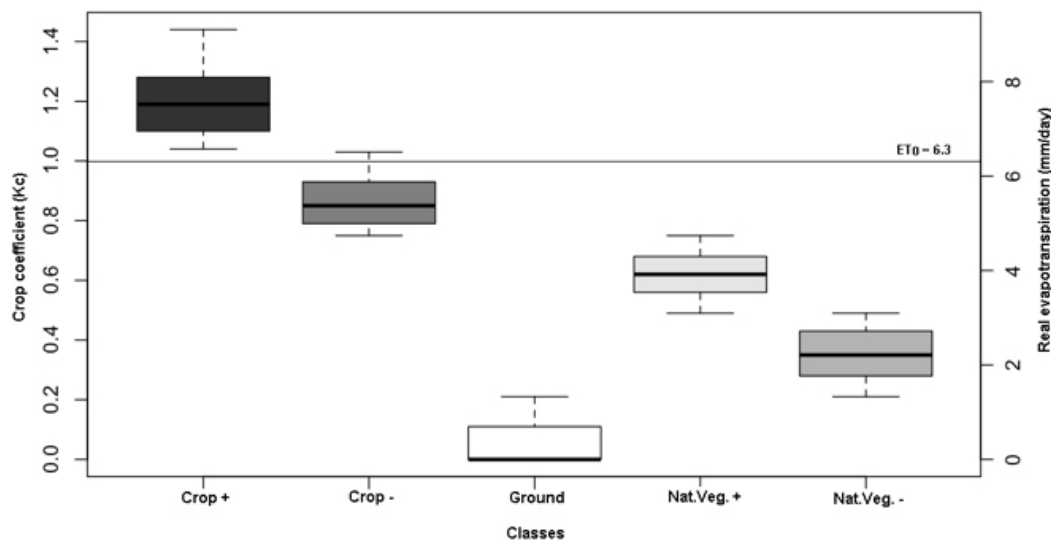


Figure 3. Kc and ETr Box plot for each classes in Paraná region (application 2).

of mean equality, indicating the existence of an effect of cover type on ETr estimated by the model. For both places, the theoretical Kc was always within the 25<sup>th</sup> and 75<sup>th</sup> percentiles, which is close to the mean and the median for all the classes. The real ET values obtained by the model are closely related to those expected for the different cover types found in the image. As expected, estimated ET values are higher than those found on surfaces that present low vegetal coverage in both locations.

In the Paraná area, mean ET was higher in crop class than in natural vegetation, and in the latter it was higher than in bare soil. Within vegetation covers, pixels classified as '+' due to their better vegetation condition (mean NDVI  $\approx 0.75$ ) and water status (lower surface temperature) showed significantly higher ETr values than those classified as '-'.

Kc values for each class found in the literature (theoretical Kc) did not differ statistically from those estimated by the model. However, a more exhaustive validation of the model can be made if the crops phenological conditions are known, with the aim of finding more accurate theoretical Kc.

Finally, the ETr was evaluated in relation to the NDVI and soil moisture (Surface temperature) to evaluate the capacity of the model to detect changes

TABLE VIII  
COEFFICIENTS OF THE SIMPLE LINEAR REGRESSION BETWEEN ETr AND NDVI, AND THEIR ASSOCIATED STATISTICS

Coefficient	t Est.	SE.	LI (95%)	LS (95%)	T	p-value
Constant	-2.36	0.08	-2.51	-2.21	-30.79	<0.0001
NDVI	10.29	0.12	10.05	10.54	82.43	<0.0001

TABLE IX  
COEFFICIENTS OF THE SIMPLE LINEAR REGRESSION BETWEEN ETr AND SURFACE TEMPERATURE, AND THEIR ASSOCIATED STATISTICS

Coefficient	Est.	S.E.	LI(95%)	LS(95%)	T	p-value
Constant	41.44	0.11	41.22	41.65	374.36	<0.0001
Temperature	-1.19	3.5E-03	-1.20	-1.18	-340.03	<0.0001

in the vegetation state and soil hydric conditions. A positive linear relationship has been found between ETr and

vegetation vigor measured (through NDVI). Nevertheless, the low fit ( $r^2 = 0.37$ ) indicates that ETr is not completely

dependent on plant state, as the capacity of a plant to absorb water can be limited due to the soil moisture content. The inverse relationship with high fit ( $r^2 = 0.91$ ) found between ETr and surface temperature, confirms this assumption.

The model presented aims to be a tool to integrate large environmental information that are permanently generated by satellite and meteorological measuring instruments. The generated script allowed us to combine procedures proposed by different authors into a single process in which the user only needs to enter crude data. The feasibility of applying models of this type to regional-scale studies is mainly limited by availability of meteorological stations. By contrast, at the site level, the limiting factor is the availability of intermediate and high resolution images with a visiting frequency that allows to describe phenological changes in crops and natural vegetation.

From the statistical analysis we conclude that the aims of the research have been satisfactorily met. The model was validated and will be useful to make estimations of evapotranspiration adjusted to site-specific variation.

#### ACKNOWLEDGMENTS

This work was carried out at CICyTTP (Diamante, Entre Ríos), ICyTE- UNMDP (Mar del Plata, Argentina) and

Regional Center of Geomatics (CEREGEO), with funds provided by Comisión Nacional de Investigaciones Científicas y Tecnológicas de la República Argentina (CONICET). The authors are especially grateful to Instituto Nacional de Tecnología Agropecuaria (INTA) and United States Geological Survey (USGS) for their free distribution policy of weather and satellite data, respectively.

#### REFERENCES

- Allen RG (2006) *Evapotranspiración del Cultivo: Guías para la Determinación de los Requerimientos de Agua de los Cultivos*. Vol. 56. United Nations Food and Agriculture Organization. Rome, Italy.
- Allen R, Tasumi M, Trezza R, Waters R, Bastiaanssen W (2002) *Sebal (Surface Energy Balance Algorithms for Land)*. Advance Training and Users Manual-Idaho Implementation, version, 1:97.
- Allen RG, Morse A, Tasumi M (2003) Application of sebal for western US water rights regulation and planning. *Proc. ICID Int. Workshop on Remote Sensing*. Montpellier, France. 15 pp.
- Allen RG, Kilic A, Suyker A, Okalebo, J (2015) Fitting measured evapotranspiration data to the fao56 dual crop coefficient method. *Proc. 2015 ASABE/IA Irrigation Symposium: Emerging Technologies for Sustainable Irrigation- A Tribute to the Career of Terry Howell*. American Society of Agricultural and Biological Engineers. pp. 1-35.
- Allen RG, Tasumi M, Trezza R (2007) Satellite-based energy balance for mapping evapotranspiration with internalized calibration (metric) model. *J. Irrig. Drain. Eng.* 133: 380-394.
- Atchley AL, Maxwell RM (2011) Influences of subsurface heterogeneity and vegetation cover on soil moisture, surface temperature and evapotranspiration at hillslope scales. *Hydrogeol. J.* 19: 289-305.
- Bannari, A., Morin, D., Benie, G., and Bonn, F. (1995). A theoretical review of different mathematical models of geometric corrections applied to remote sensing images. *Remote sensing reviews*, 13 (1-2): 27-47.
- Barsi JA, Barker JL, Schott JR (2003) An atmospheric correction parameter calculator for a single thermal band earth-sensing instrument. *Proc. IGARSS*

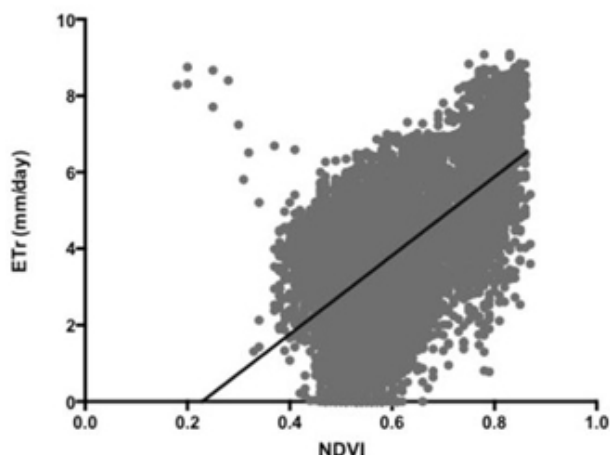


Figure 4. Real evapotranspiration as a function of NDVI for vegetation covers.  $y = -2,36 + 10,29x$ ;  $N = 11330$ ;  $R^2 = 0,37$ .

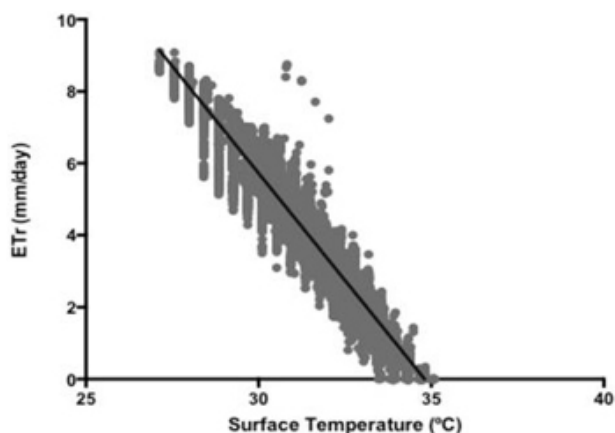


Figure 5. Real evapotranspiration as a function of surface temperature for the vegetation cover types.  $y = 41,44 - 1,19x$ ;  $N = 11330$ ;  $R^2 = 0,91$ .



2003. 2003 IEEE International Geoscience and Remote Sensing Symposium. (IEEE Cat. 03CH37477). Vol. 5: 3014-3016.
- Bastiaanssen WG (2000) Sebal-based sensible and latent heat fluxes in the irrigated gediz basin, turkey. *J. Hydrol.* 229: 87-100.
- Bastiaanssen WG, Menenti M, Feddes R, Holtslag A (1998a) A remote sensing surface energy balance algorithm for land (sebal). 1. Formulation. *J. Hydrol.* 212: 198-212.
- Bastiaanssen WG, Pelgrum H, Wang J, Ma Y, Moreno J, Roerink G, Van der Wal T (1998b) A remote sensing surface energy balance algorithm for land (sebal). 2: Validation. *J. Hydrol.* 212: 213-229.
- Berk A, Anderson GP, Bernstein LS, Acharya PK, Dothe H, Matthew MW, Adler-Golden SM, Chetwynd JH, Richtsmeier SC, Pukall B, Allred CL, Jeong LS, Hoke ML (1999) Modtran4 radiative transfer modeling for atmospheric correction. In *Optical Spectroscopic Techniques and Instrumentation for Atmospheric and Space Research III*. International Society for Optics and Photonics. Vol. 3756: 348-354.
- Blaney HF, Criddle WD (1952) *Determining Water Requirements in Irrigated Areas from Climatological and Irrigation Data*. U.S. Soil Conservation Service. 50pp.
- Brutsaert W, Sugita M (1992) Regional surface fluxes from satellite- derived surface temperatures (avhrr) and radiosonde profiles. *Bound. Layer Meteorol.* 58: 355-366.
- Chander G, Markham B (2003) Revised landsat-5 tm radiometric calibration procedures and postcalibration dynamic ranges. *IEEE Trans. Geosci. Rem. Sens.* 41: 2674-2677.
- Chuvieco E (2010) *Teledetección Ambiental: La Observación de la Tierra desde el Espacio*. Ariel. 528 pp.
- Davis RS (1992) Equation for the determination of the density of moist air (1981/91). *Metrologia* 29: 67-70.
- Duffie JA, Beckman WA, Worek W (2013) *Solar Engineering of Thermal Processes*. Vol. 3. Wiley Online. 928 pp.
- Duguay C, Ledrew E (1992) Estimating surface reflectance and albedo from landsat-5 thematic mapper over rugged terrain. *Photogram. Eng. Rem. Sens.* 58: 551-558.
- Li F, Kustas WP, Prueger JH, Neale CM, Jackson TJ (2005) Utility of remote sensing-based two-source energy balance model under low and high vegetation cover conditions. *J. Hydrometeorol.* 6: 878-891.
- Lillesand T, Kiefer RW, Chipman J (2014) *Remote Sensing and Image Interpretation*. Wiley. 736 pp.
- Markham BL, Barker JL (1986) Landsat mss and tm post-calibration dynamic ranges, exoatmospheric reflectances and at-satellite temperatures. *Landsat Tech. Notes 1*: 3-8.
- Mausser W, Schadlich S (1998) Modelling the spatial distribution of evapotranspiration on different scales using remote sensing data. *J. Hydrol.* 212: 250-267.
- Njoku EG (2014) *Encyclopedia of Remote Sensing*. Springer. 939 pp. ISBN: 978-0-387-36699-9.
- Robinove CJ, Chavez JrPS, Gehring D, Holmgren R (1981) Arid land monitoring using landsat albedo difference images. *Rem. Sen.. Environ.* 11: 133-156.
- Sanchez J, Kustas W, Caselles V, Anderson M (2008) Modelling surface energy fluxes over maize using a two-source patch model and radiometric soil and canopy temperature observations. *Rem. Sen..Environ.* 112: 1130-1143.
- Stancalie G, Nertan A (2012) Possibilities of deriving crop evapotranspiration from satellite data with the integration with other sources of information. In Irmak A (Ed.) *Evapotranspiration Remote Sensing and Modeling*. InTech. pp. 438-466.
- Sumathi S, Sivanandam S (2006) *Introduction to Data Mining and its Applications*. Vol. 29. Springer. 828 pp.
- Tan PN, Steinbach M, Kumar V (2005) *Introduction to Data Mining*. Pearson. 729pp.
- Thorntwaite CW (1948) An approach toward a rational classification of climate. *Geogr. Rev.* 38: 55-94.
- Wukelic G, Gibbons D, Martucci L, Foote H (1989) Radiometric calibration of Landsat thematic mapper thermal band. *Rem. Sens. Environ.* 28: 339-347.
- Yao Y, Liang S, Cheng J, Liu S, Fisher JB, Zhang X, Jia K, Zhao X, Qin Q, Zhao B (2013) Modis driven estimation of terrestrial latent heat flux in china based on a modified Priestley Taylor algorithm. *Agric. For. Meteorol.* 171: 187-202.
- Zeleke KT, Wade LJ (2012) Evapotranspiration estimation using soil water balance, weather and crop data. In Irmak A (Ed.) *Evapotranspiration Remote Sensing and Modeling*. InTech. pp: 41-57.
- Zeng Z, Piao S, Lin X, Yin G, Peng S, Ciais P, Myneni RB (2012) Global evapotranspiration over the past three decades: estimation based on the water balance equation combined with empirical models. *Environ. Res. Lett.* 7: 014026.